Monitoring~~ the~~ global ocean heat content from space geodetic observations to estimate the Earth energy imbalance

Florence Marti[1], Victor Rousseau[1], Michaël Ablain[1], Robin Fraudeau[1], Benoit Meyssignac[2], Alejandro Blazquez[2]

[1]Magellium, Ramonville Saint Agne, 31520, France
[2]Université de Toulouse, LEGOS, (CNES/CNRS/IRD/UT3), 31400 Toulouse~~, 31400~~, France

Correspondence to: Florence Marti (florence.marti@magellium.fr)

Abstract. ~~An~~This study presents an improved ~~spatial~~space geodetic approach ~~is presented for estimating~~to estimate the global ocean heat content (GOHC) change and the Earth energy imbalance (EEI) over 1993-2022. The ~~geodetic estimate of the~~ EEI ~~shows~~exhibits a ~~significant~~ positive trend of 0.~~75~~29 W m-2 ~~over the period 1993-2022~~decade-1, significant at the 90% confidence level, indicating accelerated ocean warming~~ of the ocean and increasing EEI~~, in line with independent CERES ~~observations. Comparisons with in situ~~ data~~ GOHC changes shows good agreement over 2005-2019. This~~. The study highlights the importance of ~~rigorously estimating~~comparing various estimates (eg. in-situ based GOHC) and their uncertainties~~ based on space geodetic data,~~ to ~~robustly~~reliably assess EEI changes.

1 Introduction

The ocean absorbs ~~much of~~almost all the excess energy stored by the Earth system that results from the anthropogenic greenhouse gas emission ~~by human activities~~ in the form of heat (~91%; ~~Church et al., 2011; Levitus et al., 2012; Meyssignac et al., 2019;~~ von Schuckmann et al., ~~2020, 2022~~2023; Foster et al., 2021). As the ocean acts as a huge heat reservoir, global ocean heat content (GOHC) is therefore a key component in the Earth's energy budget. An accurate knowledge of the GOHC change allows us to assess the Earth energy imbalance (EEI), which refers to the difference between the amount of energy the Earth receives from the sun and the amount of energy it radiates and reflects back into space. A community effort (Meyssignac et al., 2019) depicted the various methodologies to estimate EEI from the GOHC, including the use of ocean in-situ temperature and salinity profiles (von Schuckmann et al., ~~2020, 2022~~2023), the measurement of the ocean thermal expansion from space geodesy (Marti et al., 2022; Hakuba et al., 2021), ocean reanalysis (Stammer et al., 2016), and surface net flux measurements (Kato et al., 2018; L'Ecuyer et al.,~~ 2015), L'Ecuyer et al.~~ 2015). Among these approaches, the space geodetic approach, detailed in Marti et al. (2022), leverages the maturity of satellite altimetry and gravimetry measurements~~, enabling~~ to enable precise, extensive spatial and temporal coverage, and full-depth estimates of ocean thermal expansion. As the EEI magnitude is small (0.5-1.0 W m^{-2}, von Schuckmann et al., ~~2016~~2023) compared to the amount of energy entering and leaving the climate system

(~340 W m^{-2}, L'Ecuyer et al. 2015), a high level of precision and accuracy are required to estimate the EEI mean (< 0.3 W m^{-2}) and its time variations at decadal scale (< 0.1 W m^{-2}; Meyssignac et al., 2019). In this regard, the space geodetic approach emerges as a promising candidate capable of meeting the stringent EEI precision and accuracy requirements (Meyssignac et al., ~~2019; Marti et al., 2022).~~2019; Marti et al., 2022).

In this study, our primary objective is to present the updated space geodetic GOHC and EEI estimates and the improvement since Marti et al. (2022), including several major evolutions in the input data, algorithms and a temporal extension into the past, since 1993. The secondary objective is to compare this updated space geodetic monthly GOHC product with GOHC time series derived from in~~-~~-situ observations. To ensure a consistent and homogeneous treatment, we apply the same processing method to estimate the EEI from the different yearly GOHC time series considered. The obtained EEI estimates are then compared to the net flux at the top of atmosphere (TOA) derived from the Clouds and the Earth's Radiant Energy System (CERES) mission, which serves as a reference for EEI time variations.

2 Data and method

The space geodetic approach consists in deriving the ocean heat content change from the steric sea level change (i.e. the ocean expansion)~~-~~ inferred by satellite observations. We present here an update of the technique for estimating the GOHC change and the EEI, which relies on ~~the~~ existing work (Marti et al., 2022) but also benefits from the progress made more recently at regional scales (Rousseau et al., under revision).

In accordance with Rousseau et al. (under revision), the GOHC change is obtained as the sum of regional ocean heat content (OHC) estimated on a 1°x1° grid. However, the uncertainties, their characterisation and their propagation from the input data until the GOHC change and EEI are made at global scale in a similar manner to Marti et al. (2022).

Space geodetic observations are consistent with ~~the ones~~those used in Marti et al. (2022). The total sea level change is derived from altimetry sea-level gridded products data from the Copernicus Change Climate Change service (C3S) [1]. A correction for TOPEX-A drift is applied (Ablain et al., 2017) as well as a correction for the Jason-3 radiometer drift (Barnoud et al., 2023). The manometric sea level change is estimated from an update of Blazquez et al. (2018) gravimetric solution ensemble (V1.6) [2]. ~~In this update, we~~We identified a sub-sample of ~~the~~this ensemble which relies on a single geocenter correction based on Sun et al. (2016) and whose mean is used as our best estimate of the manometric sea level change.

The ~~GOHC change is obtained as the sum of regional ocean heat content (OHC) estimated on a 1°x1° grid in accordance with Rousseau et al. (under revision). The uncertainties, their characterisation and their propagation from the input data until the GOHC change and EEI are made at global scale in a similar manner to Marti et al. (2022).~~

~~Based~~space geodetic approach builds on the sea level ~~equation, space geodetic data allow estimating~~budget to estimate the steric sea level (SSL) change. ~~We derive~~ As we eventually focus on the GOHC change~~ from the SSL change neglecting, we~~ neglect the effect of the halosteric sea level change ~~(HSL)~~ because the impact of salinity changes on SSL is very small at global scale~~. Moreover, recent studies highlight that in situ salinity datasets from Argo floats - from which we are able to derive HSL change - present an instrumental drift since 2016 due to anomalies on part of the conductivity sensors (Wong et al., 2020), leading to a significant drift in the global mean HSL estimates from 2016 onwards (Barnoud et al. (2021)).~~

~~The OHC change is then~~ (see Appendix of Lowe and Gregory, 2006). The OHC change is obtained from the ratio of the SSL change and the integrated expansion efficiency of heat (IEEH) coefficient. ~~The IEEH~~Knowledge of the warming pattern is ~~computed at regional scale (1°x1°) from temperature and salinity data from the ECCO ocean reanalysis [3].~~ a prerequisite to estimate the IEEH. This knowledge relies on in-situ observations. In previous versions, the IEEH was computed ~~at global scale (Marti et al., 2022) and regional scales (Rousseau et al., under review) from in-~~ from in-situ temperature/salinity profiles (mainly Argo floats~~). The two advantages of relying on ECCO here is to extend the spatial area over which~~) (Rousseau et al., under review). Here the IEEH is computed ~~including now the coasts and the high latitudes, and~~ at regional scale (1°x1°) from temperature/salinity data from the ECCO ocean reanalysis [3]. Using ECCO to ~~take into account~~estimate the IEEH has an advantage as it allows for the expansion of the spatial area used to compute it. It now includes coastal regions up to 100km and deep ocean areas down to 6000m. ~~In this paper, we~~We have made the approximation that the IEEH is constant over time, and equals to its mean value over 2005-2015. This is justified at global scale because the heat pattern of the ocean does not change significantly on decadal time scales (Kuhlbrodt and Gregory, 2012).

~~Argo~~In-situ-derived global IEEH ranges from 1.~~45~~36 10^{-1} m YJ^{-1} for a depth down to 2000 m to 1.~~67~~57 10^{-1} m YJ^{-1} for a depth down to 6000 m. Using the ECCO ocean reanalysis [3] instead of ~~Argo~~in-situ data ~~provides~~, yields very similar global IEEH values (see Table 1). ~~The ECCO reanalysis allows to get an estimate of the global IEEH down to the bottom of the ocean and close to the coast.~~ Over ~~the entire ocean~~a larger area the ECCO reanalysis indicates an IEEH of 1.50 10^{-1} m YJ^{-1}. The global IEEH uncertainty of 1 10^{-3} m YJ^{-1} ([5%,95%] confidence interval level) is ~~obtained by considering the spread in the Argo-derived global IEEH estimates over the Argo mask (~~from Marti et al., (2022). It does not account for the IEEH variability due to the spatial domain.

In this study we propose a temporal extension of the space geodetic estimate of GOHC and EEI into the past from January 1993 ~~(at~~, the ~~beginning~~start of precise satellite altimetry~~) onwards~~. As space gravimetry observations are not available before 2002 (~~the~~ GRACE mission was launched in March 2002), the ~~global mean~~manometric sea level ~~barystatic~~ component is extended into the past with the sum of ~~the~~its individual contributions ~~to manometric sea level~~ from Greenland, Antarctica, ~~mountain~~ glaciers and from terrestrial water storage. These ~~different contributions~~ are derived from the ~~SLBC_cci product~~ESA climate change initiative assessment of the sea level budget since 1993 [4].

After calculating the GOHC, the EEI is then obtained from the time derivative of the GOHC - by applying a central finite difference scheme - and accounting for the heat fraction that is entering the ocean (~~which is~~ 91%) - the ~~rest~~remaining 9% of energy being captured by the atmosphere, land and cryosphere (Forster et al., 2021). As described in Marti et al. (2022), the OHC change needs to be filtered out beforehand by applying a Lanczos low-pass filter at 3 years to remove signals related to ocean-atmosphere exchanges which does not correspond to any response to global warmingthe top of the atmosphere radiation imbalance (Palmer and McNeall, 2014) and must therefore be removed to infer EEI variations. However, unlike Marti et al. (2022), we applied this temporal filter to regional spatial scales before summing the regional OHC estimates to obtain the GOHC. The following equation summarises how the EEI is derived from GOHC:

$$EEI(t) = \frac{dGOHC_{filtered,adjusted}(t)}{dt} \times \frac{1}{\alpha}, with \alpha with\ \alpha = 0.91 , \qquad (1)$$

It is worth noting that the impact of performing the filtering step at regional scales rather than global scale is low on the GOHC estimate, but much more significant on the EEI estimate. It is because the filtering step allows to filter out the noise before the calculation of the time derivative and thus it minimises the noise amplification in EEI induced by the time derivation.

In order to assess the GOHC and EEI estimates, the estimation of their uncertainties is a key point. Briefly, theThe method developed (described in Marti et al., 2022) consists in calculating the error variance-covariance matrices of the global mean sea level (GMSL) change data record and of the barystatic sea level data record and then propagating these error variance-covariance matrices to the GOHC and the EEI estimates. The characterisation of uncertainties is similar to that used by Marti et al. (2022). For the GMSL uncertainties, we have useduse an updated altimetry uncertainty budget provided by Guérou et al. (2022), mainly extended over the Jason-3 period (until 2021). For the barystatic sea level uncertainties, we have calculatedcalculate the dispersion of the gravimetry ensemble [2]. Note that thisThis uncertainty is not centred on the barystatic best estimate (see Figure 1). Besides, an uncertainty on the heat fraction entering the ocean has beenis introduced ([89%, 93%]) to account for%]), defined from the different estimates fromof the literature (e.g. (Church et al., 2011; Levitus et al., 2012; von Schuckmann et al., 2020; Forster et al., 2021; von Schuckmann et al., 2023). The uncertainty associated with the IEEH once propagated is negligible compared with other sources of uncertainty on the mean EEI (<0.1%). From the covariance matrices, we are able to obtain the uncertainty associated with the means, trends or accelerations in GOHC at any time scales, based on an ordinary least squaresquares regression.

The space geodetic GOHC and EEI estimates [5] have beenare then compared to other estimates mostly based on in--situ data. First, we introduce GOHC estimates based on gridded fields of temperature and salinity derived from in-situ measurements, provided by 5 centres: SIO (Scripps Institution of Oceanography) [6], JAMSTEC version 2021 [7], ISAS20 - IFREMER [8], all three relying on Argo network data; EN4 using two sets of corrections (Cheng et al., 2014; Gouretski and Cheng, 2020) [9], and NOAA (National Oceanic and Atmospheric Administration) [10]. We analyse the geodetic estimate to 32 ocean monitoring indicators (OMIs) delivered by CMEMS [611] and also based on in--situ observations (, CORA, ARMOR-3D, and hereafter "CORA-2011", CORA processed by von Schuckmann and Le Traon (2011) (later "CORA-2011"). Note that ARMOR-3D also use space measurements (altimetry and sea surface salinity and temperature) in addition to in situ observations to derive a GOHC estimate. The OMIs have been amended with a deep ocean warming estimate of +0.068 W m^{-2} from (Purkey and Johnson, 2010) to encompass the entire water column and account for the deep ocean's substantial thermal influence below 2000 m.). The CORA-2011 dataset is delivered together with an uncertainty envelope whose estimation is described in von Schuckmann and Le Traon (2011). We alsoIn addition we compare the space geodetic estimate of the GOHC to the recent Global Climate Observing System (GCOS) ensemble [7estimate [12] composed of 16 time series based on subsurface temperature measurements and representative of the full water column. For the GCOS GOHC ensemble trend we use the uncertainty indicated in von Schuckmann et al. (2023) for the period 2006-2020. Note that CORA and CORA-2011 time series are included within the GCOS ensemble. In addition, we compare the geodetic GOHC estimate with GOHC estimates derived from gridded fields of temperature and salinity products provided by 5 Argo centres, namely ISAS20 – IFREMER [8], SIO (Scripps Institution of Oceanography) [9], EN4 using two sets of corrections (Cheng et al., 2014; Gouretski and Cheng, 2020) [10], JAMSTEC version 2021 [11] and NOAA (National Oceanic and Atmospheric Administration) [12] datasets. The Argo resulting GOHC change estimates have been extended with Purkey and Johnson (2010) deep ocean contribution. It should be noted that both GCOS ensemble and OMIs are made up of yearly time series, whereas the space geodetic GOHC estimates are monthly, which restricts comparisons to interannual scales. Comparisons are thus led on the basis of annual time series, both for trend and variability study. Lastly, we introduce an alternative full-depth GOHC estimate derived from the space geodetic approach (Hakuba et al., 2021) [13] (hereafter "JPL"), whose uncertainty is obtained from an ensemble approach.

For Apart from GCOS ensemble and the EEI comparison, each of space geodetic estimates, the different GOHC change estimates are extended with a deep ocean warming estimate of +0.068 W m^{-2} from Purkey and Johnson (2010) to encompass the entire water column and account for the deep ocean's substantial thermal influence below 2000 m. In this way, all different GOHC estimates cover the whole water column down to the bottom and are thus comparable with each other.

Both GCOS ensemble and OMIs are made up of yearly time series mentioned above have been derived to obtain the , while other estimates are available on a monthly basis, which restricts comparisons to interannual time scales. Comparisons are thus led on the basis of annual time series, both for GOHC trend and EEI variability study. The GOHC change estimates are turned into EEI using the same method: annual GOHC change data as described above, with the only difference that annual time series are linearly interpolated on a monthly time scale so the derivative is made on a monthly time scale. beforehand.

The CERES Energy Balanced and Filled (EBAF) product [1314] is used as a reference for the EEI variability assessment because it is totally independent and it is known to reproduce precisely the EEI variations with uncertainties of the order of a few tenth of W.m-2.tenths of W m^{-2}. Its mean value is anchored with an in-situ product (Lyman and Johnson, 2014).

The dataDatasets used for this study are described in Table 2, both for the calculation of GOHC and EEI estimates and for their intercomparison. All uncertainties are reported in the text with a 5 %–95 % confidence level interval.

3 Results

The monthly space geodetic GOHC change (calledfrom LEGOS-Magellium) is plotted in Figure 1 from September over January 1993 to -May 2022. It highlights a trend of accumulation of heat in the ocean (86% of the total ocean surface excluding the Mediterranean sea). The trend of +0.75 W m^{-2} ~~for the whole period, providing~~provides an estimate of the global ocean heat uptake (GOHU) and ~~indicating the rate of heat accumulation in the ocean. The~~ the uncertainty range for this ~~GOHU~~accumulation rate is [0.61; 1.04] W m^{-2} meaning the GOHU is significantly positive over 1993-2022. ~~In the same figure, we also superimpose~~

A comparison is made with the annual GOHC change time series from GCOS (Figure 1). The heat content is an extensive variable and GOHC is therefore highly sensitive to spatial coverage. To ensure more consistency in comparison with GCOS, we constrained the LEGOS-Magellium dataset to an ocean surface comparable to GCOS (up to 60° latitude and for areas more than 300m deep). The impact was found to be low with a trend of 0.73 W m^{-2} over 1993-2022. Despite a higher value for the LEGOS-Magellium dataset, the trend results for 1993-2020 are in agreement within their confidence intervals, with the GCOS trend of 0.60 [0.39; 0.82] W m^{-2} and the LEGOS-Magellium trend of 0.71 [0.58, 0.99] W m^{-2}.

~~The area covered by both datasets is not identical with differences in coastal areas (areas less than 100 km from the coast are excluded for spatial geodetic data, while a 300 m bathymetry criterion is applied for each GCOS ensemble member) and also in latitudes (GCOS members are limited to the latitude 60° while the geodetic method goes up to 66°). As a result, GCOS solutions are derived from data spanning 76% of the total ocean surface, while the geodetic approach covers 87%. As OHC is an integrative variable, the GOHC change estimates are very sensitive to spatial coverage which may explain some differences in trend at global scale. Over their respective area of data availability, the trend of GCOS OHC ensemble is lower (0.60 [0.39; 0.82]), but still in agreement with the space geodetic within their confidence interval (0.73 [0.59; 1.02]). When considering the same spatial extension as the GCOS ensemble, the space geodetic GOHC trend drops to 0.62 [0.50; 0.88] W m^{-2} and is closer to that of the GCOS ensemble.~~

~~We compare the geodetic GOHC trends with all the other estimates (Figure 2) over the common period of availability 2005-2019. In a general manner the space-geodetic approach shows a more pronounced trend in GOHC than approaches based on in situ data (Hakuba et al., 2021). GOHC estimates based on Argo show also smaller uncertainty in general. However, although GOHC estimates based on Argo are built from the same temperature and salinity Argo profiles, they show some differences that are due to the processing (e.g. selection of valid profiles, gridding algorithm, etc…). Note that the area considered for the Argo-based GOHC change calculation corresponds to the Argo mask, defined in Table 1 and covering 79% of the ocean surface while the geodetic approach is using the altimetry mask that covers 87% of the ocean.~~

~~Figure 3 shows the temporal~~When the GOHC trends are calculated over a shorter period (2005-2019) on their respective available ocean surface (Figure 2), the conclusions are similar to those in Figure 1. GOHC trend results from other estimates are also shown. Note that the GCOS ensemble encompasses CORA and CORA-2011 datasets as well as solutions based on the same in-situ temperature and salinity grids that are used and mentioned in section 2. In general, GOHC estimates exclusively based on in-situ measurements are in agreement within their uncertainty ranges. These estimates are constructed using the same atlas of temperature and salinity profiles. Specifically, the data used to calculate the 5 GOHC from gridded fields covers the same ocean surface. Despite this, their trends show some discrepancies that are due to the data processing such as the selection of valid profiles and gridding algorithm. The comparisons confirm that the LEGOS-Magellium dataset shows a stronger trend in GOHC than datasets relying on in-situ measurements, but still agrees within the 90% confidence level. The JPL space geodetic estimate supports these results and increases our confidence in our method.

Temporal variations of the EEI derived from the monthly LEGOS-Magellium space geodetic dataset ~~as~~agree well ~~as that obtained from the GCOS yearly ensemble and~~with the direct EEI measurements provided by CERES~~.~~ but less so with the EEI derived from the GCOS yearly ensemble (Figure 3). Correlated signals are observed, particularly after 2006. These interannual variations are related to the main coupled ocean-atmosphere climate modes modes such as El Niño or the Pacific Decadal Oscillation (Loeb et al. 2018,Meyssignac et al., 2023) or the atmospheric aerosol content resulting from volcanic eruptions and anthropogenic emissions. The 3 EEI solutions ~~detect~~show a trend ~~in EEI~~ over their respective ~~period~~periods: 0.29 [0.04;0.56] W m^{-2} $decade^{-1}$ for LEGOS-Magellium over 1993-2022; ~~-~~0.~~16~~17 W m^{-2} $decade^{-1}$ [-0.~~19;~~25;0.60] for GCOS over 1993-2020; 0.~~51] for GCOS over 1993-2020; 0.46~~44 [0.34; 0.~~59~~55] W m^{-2} $decade^{-1}$ for CERES over 2000-2022. ~~When considering~~Over the common period 2000-2020~~ period,~~, the LEGOS~~ and ~~-Magellium dataset shows a positive trend of 0.~~39~~37 W m^{-2} $decade^{-1}$ in agreement with CERES EEI trend of 0.44 W m^{-2} $decade^{-1}$ ~~that is closer to the 0.49 W m^{-2} $decade^{-1}$ trend of CERES over the same period~~and both trends are significant at the 90% confidence level. Given the confidence intervals and good agreement between these independent datasets, these results provide confidence in the observed trend in EEI since 2000, indicating a very likely acceleration in global ocean warming over ~~the periods specified. The Taylor diagram in Figure 4 indicates the similarity in terms of temporal variability of all EEI products with the CERES reference. The proximity of a dataset to the blue star determines the degree of agreement and how well the dataset matches CERES estimate of the EEI variability. The GCOS and LEGOS-Magellium products show close time variations with a correlation of approximately 0.7. The ARMOR-3D product has the highest correlation (0.84) but also a significant standard deviation. The Argo-based products range from 0.22 to 0.79 in correlation, indicating varying levels of agreement with CERES.~~2000-2020.

The Taylor diagram in Figure 4 indicates the similarity in terms of temporal variability between all OHC-based EEI and the CERES reference. The dataset's proximity to the blue star determines the degree of agreement and how well it matches CERES estimate of the EEI variability. The GCOS and LEGOS-Magellium products exhibit similar time variations, with a correlation of approximately 0.7, which is comparable to the results of Loeb et al. (2021). The JPL EEI has the highest correlation with CERES data (0.9), but too much variability. In-situ-based products have a correlation range of 0.25 to 0.8, indicating different levels of agreement with CERES.

4 Discussions and conclusions

~~In this~~This study ~~we propose~~proposes an extended estimate of the GOHC change and the EEI from 1993 onwards ~~based on~~using the space geodetic approach~~ and we~~. We compare ~~it~~ this estimate with various estimates based on in-situ measurements, as well as with the CERES EBAF estimate of the EEI~~ and~~.

Apart from ~~various estimates based on Argo in situ measurements.~~

Mi

~~The~~the global measurement by CERES, the studied methods do not yet cover the entire ocean. However, the major advantage of the space geodetic approach is ~~to take into account the~~ the large and homogeneous sampling of the ocean surface since August 2002, and the integration of the whole water column~~, thanks to the integrated observations of space~~. The space geodetic GOHC shows a significant trend of +0.75 [0.61;1.04] W m^{-2} and EEI trend of 0.29 [0.04;0.56] W m^{-2} $decade^{-1}$ over the period 1993-2022.

Considering the current knowledge of the uncertainties associated with satellite gravimetry and altimetry ~~since 2002. Comparing space geodetic GOHC~~ data, the comparison of our results with other ~~data sets, mainly based on in situ temperature and salinity profile data of the Argo network, has allowed~~datasets allows us to cross-check the consistency of the different estimates~~. Over the period 1993-2022, the spatial geodetic GOHC shows a significant trend of +0.75 [0.61;1.04] W m^{-2}. Over 2005-2019 the geodetic estimate of GOHC trend is slightly higher than Argo based estimates at the 66%~~ of the ocean warming rate within a [5%-95%] confidence level ~~but it is in general agreement at the 90% confidence level. Besides the difference in spatial coverage of the input data, the discrepancy observed at the 66% confidence level~~interval. However, the higher GOHC trends observed with the space geodetic approach (LEGOS-Magellium and JPL datasets) compared to all in-situ datasets could reveal limitations in the observing systems such as the unobserved deep ocean with in~~-~~-situ data or systematic errors in ~~spatial~~space geodetic data, which need to be further investigated.

In addition, the comparison of ~~the~~our space geodetic EEI estimate with the direct EEI estimates provided by the CERES EBAF dataset provides complementary assessment information on the variability of EEI. On the one hand we find a good temporal correlation of the EEI derived from space geodetic and CERES EBAF ~~estimate~~estimates. On the other hand a significant EEI trend has been detected in both CERES and the space geodetic approach suggesting a very likely acceleration of ~~current~~ global ocean warming~~. This study also highlights~~ over the ~~rigorous estimation of uncertainties and their propagation from space geodetic data, based on a mature and advanced state of knowledge of altimetric and gravimetric measurements~~last 20 years.

Data availability

Space geodetic GOHC change and EEI dataset (v5.0) is available online at https://doi.org/10.24400/527896/a01-2020.003 (Magellium/LEGOS, 2020) with the complete associated documentation (product user manual and algorithm theoretical basis document).

Acknowledgements

We would like to first thank Audrey Minière, Karina Von Schuckmann and Lorena Moreira Mendez for their contributions to the preparation of this paper and Françoise Mertz for making the data available on the ODATIS portal and AVISO. We also thank two anonymous reviewers for their constructive comments on earlier drafts of this manuscript.

Financial support

This work has been supported by CNES, both for its development and dissemination. Comparison with other datasets was funded by CNRS. ESA initially supported this work in the framework of the MOHeaCAN project (Monitoring Ocean Heat Content and Earth Energy ImbalANce from Space): https://eo4society.esa.int/projects/moheacan/ (last access: 20 December 2023).

Competing interests

The contact author has declared that none of the authors has any competing interests.

References

Ablain, M., Jugier, R., Zawadki, L., Taburet, N., Cazenave, A., and Meyssignac, B.: The TOPEX-A Drift and Impacts on GMSL Time Series, AVISO Website, October 2017, 2017.

~~Barnoud, A., Pfeffer, J., Guérou, A., Frery, M.-L., Siméon, M., Cazenave, A., Chen, J., Llovel, W., Thierry, V., Legeais, J.-F., and Ablain, M.: Contributions of altimetry and Argo to non-closure of the global mean sea level budget since 2016, Geophys. Res. Lett., https://doi.org/10.1029/2021gl092824, 2021.~~

Barnoud, A., Picard, B., Meyssignac, B., Marti, F., Ablain, M., and Roca, R.: Reducing the Uncertainty in the Satellite Altimetry Estimates of Global Mean Sea Level Trends Using Highly Stable Water Vapor Climate Data Records, J. Geophys. Res. Oceans, 128, e2022JC019378, https://doi.org/10.1029/2022JC019378, 2023.

Blazquez, A., Meyssignac, B., Lemoine, J., Berthier, E., Ribes, A., and Cazenave, A.: Exploring the uncertainty in GRACE estimates of the mass redistributions at the Earth surface: implications for the global water and sea level budgets, Geophys. J. Int., 215, 415–430, https://doi.org/10.1093/gji/ggy293, 2018.

Cheng, L., Zhu, J., Cowley, R., Boyer, T., and Wijffels, S.: Time, probe type, and temperature variable bias corrections to historical expendable bathythermograph observations, J. Atmospheric Ocean. Technol., 31, 1793–1825, 2014.

Church, J. A., White, N. J., Konikow, L. F., Domingues, C. M., Cogley, J. G., Rignot, E., Gregory, J. M., Broeke, M. R. van den, Monaghan, A. J., and Velicogna, I.: Revisiting the Earth's sea-level and energy budgets from 1961 to 2008, Geophys. Res. Lett., 38, https://doi.org/10.1029/2011GL048794, 2011.

Consortium, E., Fukumori, I., Wang, O., Fenty, I., Forget, G., Heimbach, P., and Ponte, R. M.: Synopsis of the ECCO Central Production Global Ocean and Sea-Ice State Estimate, Version 4 Release 4, Zenodo, https://doi.org/10.5281/zenodo.4533349, 2021.

DOELLING, D. R.: CERES Energy Balanced and Filled (EBAF) TOA and Surface Monthly means data in netCDF Edition 4.2, https://doi.org/10.5067/TERRA-AQUA-NOAA20/CERES/EBAF_L3B004.2, 2023.

ECCO Consortium, Fukumori, I., Wang, O., Fenty, I., Forget, G., Heimbach, P., & Ponte, R. M. (2023). ECCO Central

Estimate (Version 4 Release 4). Retrieved from https://www.ecco-group.org/products-ECCO-V4r4.htm, last access: 14 July 2023

Forget, G., Campin, J.-M., Heimbach, P., Hill, C., Ponte, R., and Wunsch, C.: ECCO version 4: An integrated framework for non-linear inverse modeling and global ocean state estimation, Geosci. Model Dev., 8, 3071–3104, 2015.

Forster, P., Storelvmo, T., Armour, K., Collins, W., Dufresne, J.-L., Frame, D., Lunt, D., Mauritsen, T., Palmer, M., and Watanabe, M.: The Earth's energy budget, climate feedbacks, and climate sensitivity, 2021.

Foster, J., Smallcombe, J. W., Hodder, S., Jay, O., Flouris, A. D., Nybo, L., and Havenith, G.: An advanced empirical model for quantifying the impact of heat and climate change on human physical work capacity, Int. J. Biometeorol., 65, 1215–1229, https://doi.org/10.1007/s00484-021-02105-0, 2021.

Gaillard, F., Reynaud, T., Thierry, V., Kolodziejczyk, N., and Schuckmann, K. von: In Situ–Based Reanalysis of the Global Ocean Temperature and Salinity with ISAS: Variability of the Heat Content and Steric Height, J. Clim., 29, 1305–1323, https://doi.org/10.1175/JCLI-D-15-0028.1, 2016.

Garcia, H. E., Boyer, T. P., Baranova, O. K., Locarnini, R. A., Mishonov, A. V., and Grodsky, A.: World ocean atlas 2018: Product documentation., 2019.

Good, S. A., Martin, M. J., and Rayner, N. A.: EN4: Quality controlled ocean temperature and salinity profiles and monthly objective analyses with uncertainty estimates, J. Geophys. Res. Oceans, 118, 6704–6716, https://doi.org/10.1002/2013JC009067, 2013.

Gouretski, V. and Cheng, L.: Correction for systematic errors in the global dataset of temperature profiles from mechanical bathythermographs, J. Atmospheric Ocean. Technol., 37, 841–855, 2020.

Guérou, A., Meyssignac, B., Prandi, P., Ablain, M., Ribes, A., and Bignalet-Cazalet, F.: Current observed global mean sea level rise and acceleration estimated from satellite altimetry and the associated uncertainty, All Depths/Remote Sensing/All Geographic Regions/Sea level/Oceans and climate, https://doi.org/10.5194/egusphere-2022-330, 2022.

Hakuba, M. Z., Frederikse, T., and Landerer, F. W.: Earth's Energy Imbalance From the Ocean Perspective (2005–2019), Geophys. Res. Lett., 48, e2021GL093624, https://doi.org/10.1029/2021GL093624, 2021.

Horwath, M., Gutknecht, B. D., Cazenave, A., Palanisamy, H. K., Marti, F., Marzeion, B., Paul, F., Le Bris, R., Hogg, A. E., Otosaka, I., Shepherd, A., Döll, P., Cáceres, D., Müller Schmied, H., Johannessen, J. A., Nilsen, J. E. Ø., Raj, R. P., Forsberg, R., Sandberg Sørensen, L., Barletta, V. R., Simonsen, S., Knudsen, P., Andersen, O. B., Ranndal, H., Rose, S. K., Merchant, C. J., Macintosh, C. R., Von Schuckmann, K., Novotny, K., Groh, A., Restano, M., and Benveniste, J.: ESA Sea Level Budget Closure Climate Change Initiative (SLBC_cci): Time series of global mean sea level budget and ocean mass budget elements (1993-2016, at monthly resolution), version 2.2, https://doi.org/10.5285/17C2CE31784048DE93996275EE976FFF, 2021.

Horwath, M., Gutknecht, B. D., Cazenave, A., Palanisamy, H. K., Marti, F., Marzeion, B., Paul, F., Bris, R. L., Hogg, A. E., Otosaka, I., Shepherd, A., Döll, P., Cáceres, D., Schmied, H. M., Johannessen, J. A., Nilsen, J. E. Ø., Raj, R. P., Forsberg, R., Sørensen, L. S., Barletta, V. R., Simonsen, S. B., Knudsen, P., Andersen, O. B., Randall, H., Rose, S. K., Merchant, C. J., Macintosh, C. R., Schuckmann, K. von, Novotny, K., Groh, A., Restano, M., and Benveniste, J.: Global sea-level budget and ocean-mass budget, with focus on advanced data products and uncertainty characterisation, Earth Syst. Sci. Data, 14, 411–447, https://doi.org/10.5194/essd-14-411-2022, 2022.

Hosoda, S., Ohira, T., Sato, K., and Suga, T.: Improved description of global mixed-layer depth using Argo profiling floats, J. Oceanogr., 66, 773–787, https://doi.org/10.1007/s10872-010-0063-3, 2010.

Kato, S., Rose, F. G., Rutan, D. A., Thorsen, T. J., Loeb, N. G., Doelling, D. R., Huang, X., Smith, W. L., Su, W., and Ham, S.-H.: Surface Irradiances of Edition 4.0 Clouds and the Earth's Radiant Energy System (CERES) Energy Balanced and Filled (EBAF) Data Product, J. Clim., 31, 4501–4527, https://doi.org/10.1175/JCLI-D-17-0523.1, 2018.

Kolodziejczyk, N., Prigent-Mazella, A., and Gaillard, F.: ISAS temperature and salinity gridded fields, https://doi.org/10.17882/52367, 2021.

Kuhlbrodt, T. and Gregory, J. M.: Ocean heat uptake and its consequences for the magnitude of sea level rise and climate change, Geophys. Res. Lett., 39, https://doi.org/10.1029/2012GL052952, 2012.

L'Ecuyer, T. S., Beaudoing, H. K., Rodell, M., Olson, W., Lin, B., Kato, S., Clayson, C. A., Wood, E., Sheffield, J., Adler, R., Huffman, G., Bosilovich, M., Gu, G., Robertson, F., Houser, P. R., Chambers, D., Famiglietti, J. S., Fetzer, E., Liu, W. T., Gao, X., Schlosser, C. A., Clark, E., Lettenmaier, D. P., and Hilburn, K.: The Observed State of the Energy Budget in the Early Twenty-First Century, J. Clim., 28, 8319–8346, https://doi.org/10.1175/JCLI-D-14-00556.1, 2015.

Legeais, J.-F., Meyssignac, B., Faugère, Y., Guerou, A., Ablain, M., Pujol, M.-I., Dufau, C., and Dibarboure, G.: Copernicus Sea Level Space Observations: A Basis for Assessing Mitigation and Developing Adaptation Strategies to Sea Level Rise, Front. Mar. Sci., 8, 2021.

Levitus, S., Antonov, J. I., Boyer, T. P., Locarnini, R. A., Garcia, H. E., and Mishonov, A. V.: Global ocean heat content 1955-2008 in light of recently revealed instrumentation problems: GLOBAL OCEAN HEAT CONTENT, Geophys. Res. Lett., 36, n/a-n/a, https://doi.org/10.1029/2008GL037155, 2009.

Levitus, S., Antonov, J. I., Boyer, T. P., Baranova, O. K., Garcia, H. E., Locarnini, R. A., Mishonov, A. V., Reagan, J. R., Seidov, D., Yarosh, E. S., and Zweng, M. M.: World ocean heat content and thermosteric sea level change (0–2000 m), 1955–2010, Geophys. Res. Lett., 39, https://doi.org/10.1029/2012GL051106, 2012.

Loeb, N. G., Doelling, D. R., Wang, H., Su, W., Nguyen, C., Corbett, J. G., Liang, L., Mitrescu, C., Rose, F. G., and Kato, S.: Clouds and the Earth's Radiant Energy System (CERES) Energy Balanced and Filled (EBAF) Top-of-Atmosphere (TOA) Edition-4.0 Data Product, J. Clim., 31, 895–918, https://doi.org/10.1175/JCLI-D-17-0208.1, 2018.

Lopez, A.: Sea level daily gridded data from satellite observations for the global ocean from 1993 to present, https://doi.org/10.24381/CDS.4C328C78, 2018.

Lowe, J. A. and Gregory, J. M.: Understanding projections of sea level rise in a Hadley Centre coupled climate model, J. Geophys. Res. Oceans, 111, https://doi.org/10.1029/2005JC003421, 2006.

Lyman, J. M. and Johnson, G. C.: Estimating global ocean heat content changes in upper 1800 m since 1950 and the influence of climatology choice, J. Clim., 27, 1945–1957, https://doi.org/10.1175/JCLI-D-12-00752.1, 2014.

Magellium/LEGOS: Climate indicators from space: Ocean heat content and Earth energy imbalance (V5V1-0), AVISO [data set], https://doi.org/10.24400/527896/A01-2020.003, 2020.

Marti, F., Blazquez, A., Meyssignac, B., Ablain, M., Barnoud, A., Fraudeau, R., Jugier, R., Chenal, J., Larnicol, G., Pfeffer, J., Restano, M., and Benveniste, J.: Monitoring the ocean heat content change and the Earth energy imbalance from space altimetry and space gravimetry, Earth Syst. Sci. Data, 14, 229–249, https://doi.org/10.5194/essd-14-229-2022, 2022.

Meyssignac, B., Boyer, T., Zhao, Z., Hakuba, M. Z., Landerer, F. W., Stammer, D., Köhl, A., Kato, S., L'Ecuyer, T., Ablain, M., Abraham, J. P., Blazquez, A., Cazenave, A., Church, J. A., Cowley, R., Cheng, L., Domingues, C. M., Giglio, D., Gouretski, V., Ishii, M., Johnson, G. C., Killick, R. E., Legler, D., Llovel, W., Lyman, J., Palmer, M. D., Piotrowicz, S., Purkey, S. G., Roemmich, D., Roca, R., Savita, A., Schuckmann, K. von, Speich, S., Stephens, G., Wang, G., Wijffels, S. E., and Zilberman, N.: Measuring Global Ocean Heat Content to Estimate the Earth Energy Imbalance, Front. Mar. Sci., 6, https://doi.org/10.3389/fmars.2019.00432, 2019.

Meyssignac, B., Chenal, J., Loeb, N., Guillaume-Castel, R., and Ribes, A.: Time-variations of the climate feedback parameter λ are associated with the Pacific Decadal Oscillation, Commun. Earth Environ., 4, 1–10, https://doi.org/10.1038/s43247-023-00887-2, 2023.

Monier, M., Derval, C., and Fernandez, E.: EU Copernicus Marine Service Product User Manual for the Global Ocean Heat Content (0-2000m) time series and trend from Reanalysis & Multi-Observations Reprocessing, GLOBAL_OMI_OHC_area_averaged_anomalies_0_2000, Issue 4.0, Mercator Ocean International, https://catalogue.marine.copernicus.eu/documents/PUM/CMEMS-OMI-PUM-GLO-OHC.pdf, last access: 14 July 2023, 2021.

Palmer, M. D. and McNeall, D. J.: Internal variability of Earth's energy budget simulated by CMIP5 climate models, Environ. Res. Lett., 9, 034016, https://doi.org/10.1088/1748-9326/9/3/034016, 2014.

Purkey, S. G. and Johnson, G. C.: Warming of Global Abyssal and Deep Southern Ocean Waters between the 1990s and 2000s: Contributions to Global Heat and Sea Level Rise Budgets, J. Clim., 23, 6336–6351, https://doi.org/10.1175/2010JCLI3682.1, 2010.

Roemmich, D. and Gilson, J.: The 2004–2008 mean and annual cycle of temperature, salinity, and steric height in the global ocean from the Argo Program, Prog. Oceanogr., 82, 81–100, https://doi.org/10.1016/j.pocean.2009.03.004, 2009.

Rousseau, V., Fraudeau, R., Hammond, M., Houndegnonto, O. J., Ablain, M., Blazquez, A., Calafat, F. M., Desbruyères, D., Foti, G., Llovel, W., Marti, F., Meyssignac, B., Restano, M., and Benveniste, J.: Monitoring the regional Ocean Heat Content change over the Atlantic Ocean with the space geodetic approach, Earth Syst. Sci. Data, under review.

von Schuckmann, K. and Le Traon, P.-Y.: How well can we derive Global Ocean Indicators from Argo data?, Ocean Sci., 7, 783–791, https://doi.org/10.5194/os-7-783-2011, 2011.

von Schuckmann, K., Palmer, M. D., Trenberth, K. E., Cazenave, A., Chambers, D., Champollion, N., Hansen, J., Josey, S. A., Loeb, N., Mathieu, P.-P., Meyssignac, B., and Wild, M.: An imperative to monitor Earth's energy imbalance, Nat. Clim. Change, 6, 138, 2016.

~~von Schuckmann, K., Cheng, L., Palmer, M. D., Hansen, J., Tassone, C., Aich, V., Adusumilli, S., Beltrami, H., Boyer, T., Cuesta-Valero, F. J., Desbruyères, D., Domingues, C., García-García, A., Gentine, P., Gilson, J., Gorfer, M., Haimberger, L., Ishii, M., Johnson, G. C., Killick, R., King, B. A., Kirchengast, G., Kolodziejczyk, N., Lyman, J., Marzeion, B., Mayer, M., Monier, M., Monselesan, D. P., Purkey, S., Roemmich, D., Schweiger, A., Seneviratne, S. I., Shepherd, A., Slater, D. A., Steiner, A. K., Straneo, F., Timmermans, M.-L., and Wijffels, S. E.: Heat stored in the Earth system: where does the energy go?, Earth Syst. Sci. Data, 12, 2013–2041, https://doi.org/10.5194/essd-12-2013-2020, 2020.~~

~~von Schuckmann, K~~., Monier, M., and Drevillon, M.: EU Copernicus Marine Service Quality Information Document for the Global Ocean Heat Content (0-2000m) time series and trend from Reanalysis & Multi-Observations Reprocessing, GLOBAL_OMI_OHC_area_averaged_anomalies_0_2000, Issue 1.0, Mercator Ocean International, https://catalogue.marine.copernicus.eu/documents/QUID/CMEMS-OMI-QUID-GLO-OHC.pdf, last access: 14 July 2023, 2021.

von Schuckmann, K. and Le Traon, P.-Y.: How well can we derive Global Ocean Indicators from Argo data?, Ocean Sci., 7, 783–791, https://doi.org/10.5194/os-7-783-2011, 2011.

von Schuckmann, K., Minière, A., Gues, F., Cuesta-Valero, F. J., Kirchengast, G., Adusumilli, S., Straneo, F., Allan, R., Barker, P. M., Beltrami, H., Boyer, T., Cheng, L., Church, J., Desbruyeres, D., Dolman, H., Domingues, C., García-García, A., Giglio, D., Gilson, J., Gorfer, M., Haimberger, L., Hendricks, S., Hosoda, S., Johnson, G. C., Killick, R., King, B. A., Kolodziejczyk, N., Korosov, A., Krinner, G., Kuusela, M., Langer, M., Lavergne, T., Li, Y., Lyman, J., Marzeion, B., Mayer, M., MacDougall, A., Lawrence, I., McDougall, T., Monselesan, D. P., Nitzbon, J., Otosaka, I., Peng, J., Purkey, S., Roemmich, D., Sato, K., Sato, K., Savita, A., Schweiger, A., Shepherd, A., Seneviratne, S. I., Simons, L., Slater, D. A., Slater, T., Smith, N., Steiner, A. K., Suga, T., Szekely, T., Thiery, W., Timmermanns, M.-L., Vanderkelen, I., Wijffels, S. E., Wu, T., and Zemp, M.: Heat stored in the Earth system 1960-2020: Where does the energy go?, 2022.

von Schuckmann, K., Minière, A., Gues, F., Cuesta-Valero, F. J., Kirchengast, G., Adusumilli, S., Straneo, F., Ablain, M., Allan, R. P., Barker, P. M., Beltrami, H., Blazquez, A., Boyer, T., Cheng, L., Church, J., Desbruyeres, D., Dolman, H., Domingues, C. M., García-García, A., Giglio, D., Gilson, J. E., Gorfer, M., Haimberger, L., Hakuba, M. Z., Hendricks, S., Hosoda, S., Johnson, G. C., Killick, R., King, B., Kolodziejczyk, N., Korosov, A., Krinner, G., Kuusela, M., Landerer, F. W., Langer, M., Lavergne, T., Lawrence, I., Li, Y., Lyman, J., Marti, F., Marzeion, B., Mayer, M., MacDougall, A. H., McDougall, T., Monselesan, D. P., Nitzbon, J., Otosaka, I., Peng, J., Purkey, S., Roemmich, D., Sato, K., Sato, K., Savita, A., Schweiger, A., Shepherd, A., Seneviratne, S. I., Simons, L., Slater, D. A., Slater, T., Steiner, A. K., Suga, T., Szekely, T., Thiery, W., Timmermans, M.-L., Vanderkelen, I., Wjiffels, S. E., Wu, T., and Zemp, M.: Heat stored in the Earth system 1960–2020: where does the energy go?, Earth Syst. Sci. Data, 15, 1675–1709, https://doi.org/10.5194/essd-15-1675-2023, 2023.

Stammer, D., Balmaseda, M., Heimbach, P., Köhl, A., and Weaver, A.: Ocean Data Assimilation in Support of Climate Applications: Status and Perspectives, Annu. Rev. Mar. Sci., 8, 491–518, https://doi.org/10.1146/annurev-marine-122414-034113, 2016.

Sun, Y., Riva, R., and Ditmar, P.: Optimizing estimates of annual variations and trends in geocenter motion and J2 from a combination of GRACE data and geophysical models, J. Geophys. Res. Solid Earth, 121, 8352–8370, https://doi.org/10.1002/2016JB013073, 2016.

~~Wong, A. P. S., Wijffels, S. E., Riser, S. C., Pouliquen, S., Hosoda, S., Roemmich, D., Gilson, J., Johnson, G. C., Martini, K., Murphy, D. J., Scanderbeg, M., Bhaskar, T. V. S. U., Buck, J. J. H., Merceur, F., Carval, T., Maze, G., Cabanes, C., André, X., Poffa, N., Yashayaev, I., Barker, P. M., Guinehut, S., Belbéoch, M., Ignaszewski, M., Baringer, M. O., Schmid, C., Lyman, J. M., McTaggart, K. E., Purkey, S. G., Zilberman, N., Alkire, M. B., Swift, D., Owens, W. B., Jayne, S. R., Hersh, C., Robbins, P., West-Mack, D., Bahr, F., Yoshida, S., Sutton, P. J. H., Cancouët, R., Coatanoan, C., Dobbler, D., Juan, A. G., Gourrion, J., Kolodziejczyk, N., Bernard, V., Bourlès, B., Claustre, H., D'Ortenzio, F., Le Reste, S., Le Traon, P.-Y., Rannou, J.-P., Saout-Grit, C., Speich, S., Thierry, V., Verbrugge, N., Angel-Benavides, I. M., Klein, B., Notarstefano, G., Poulain, P.-M., Vélez-Belchí, P., Suga, T., Ando, K., Iwasaska, N., Kobayashi, T., Masuda, S., Oka, E., Sato, K., Nakamura, T., Sato, K., Takatsuki, Y., Yoshida, T., Cowley, R., Lovell, J. L., Oke, P. R., van Wijk, E. M., Carse, F., Donnelly, M., Gould, W. J., Gowers, K., King, B. A., Loch, S. G., Mowat, M., Turton, J., Rama Rao, E. P., Ravichandran, M., Freeland, H. J., Gaboury, I., Gilbert, D., Greenan, B. J. W., Ouellet, M., Ross, T., Tran, A., Dong, M., Liu, Z., Xu, J., Kang, K., Jo, H., et al.: Argo Data 1999–2019: Two Million Temperature-Salinity Profiles and Subsurface Velocity Observations From a Global Array of Profiling Floats, Front. Mar. Sci., 7, 2020.~~

Table 1: Impact of the depth and the geographical ~~mask~~extent considered ~~in~~for the global integrated expansion efficiency of heat (IEEH) coefficient derived from ~~Argo~~ECCO reanalysis and ~~ECCO~~in-situ data (~~Argo mask~~ISAS20 [8] over 0-2000m and EN4.2.2.l09 [15] for the 2000-6000m layer). The term 'GCOS' in this context refers to the ~~most restrictive Argo geographical mask among Argo products see Fig. 1 in Marti et al. (2022)).~~domain on which the Global Climate Observing System ensemble [12] described in von Schuckmann et al. (2023) is estimated. The table presents IEEH values estimated over a comparable extent, with the notable difference being the exclusion of the Mediterranean.

Geographical area and depth	Value of the IEEH coefficient at global scale over the 2005-2015 period (unit: m YJ^{-1})	
	~~Argo~~In-situ	**ECCO**

~~Argo mask~~Spatial extent comparable to GCOS, 2000m	0.~~145~~136	0.~~145~~135
~~Argo mask~~Spatial extent comparable to GCOS, 6000m	0.~~167~~157	0.~~168~~156
~~Extension~~Spatial extension near coasts - LEGOS-Magellium dataset V5.0, 6000m	Not available	0.150

Table 2: Data used to calculate the space geodetic ocean heat content change and Earth energy imbalance and to perform comparisons.

Product ref No	Product ID & type	Data access	Reference
1	Sea level gridded data from satellite observations for the global ocean from 1993 to present.-	EU Copernicus Climate Change Service, (2018)	Dataset : Lopez, 2018 Publication: Legeais et al. (2021)
2	LEGOS gravimetric (GRACE, GRACE-FO) ensemble of manometric sea level solutions.	LEGOS FTP site: http://ftp.legos.obs-mip.fr/pub/soa/gravimetrie/grace_legos/V1.6/	Update of Blazquez et al., (2018)
3	Estimating the Circulation and the Climate of the Ocean - Central Production Version 4 Release 4 (ECCOv4r4)	NASA ECCO-group website	Dataset: ~~ECCO~~ Consortium et al., 2023.- Publication: Forget et al., 2015; Consortium et al., 2021.
4	Mass contributions to global mean sea level - ~~data set~~dataset of the European Space Agency Sea Level Budget Closure Climate Change Initiative (SLBC_cci)	CEDA archive	Dataset: Horwath et al., 2021.- Publication: Horwath et al., 2022
5	LEGOS-Magellium GOHC change/EEI dataset, v5.0	CNES AVISO website	Dataset: Magellium/LEGOS, 2020 Documentation: Algorithm Theoretical Basis- ~~Publication: update of~~ Document and Product User Manual
6	Scripps institution of oceanography (SIO) - Roemmich-Gilson Argo Climatology~~GLOBAL_OMI_OHC_area_averaged_anomalies_0_2000; Numerical models, In-situ observations, Satellite observations~~	UCSD SIO Argo website: https://sio-argo.ucsd.edu/RG_Climatology.html ~~EU Copernicus Marine Service Product, 2021.~~	~~Quality Information Document (QUID): von Schuckmann et al., 2021.~~ Publication: Roemmich and Gilson, 2009~~Product User Manual (PUM): Monier et al., 2021~~

7	JAMSTEC Argo product - Grid Point Value of the Monthly Objective Analysis using the Argo data (MOAA GPV), version 2021~~GCOS EHI Experiment 1960-2020~~	JAMSTEC website : https://www.jamstec.go.jp/argo_research/dataset/moaagpv/moaa_en.html~~World Data Center for Climate at DKRZ~~	~~Dataset: von Schuckmann et al., 2022.~~ Publication: ~~von Schuckmann~~Hosoda et al., ~~2023.~~2010
8	ISAS20 temperature and salinity gridded fields	SEANOE - Sea Scientific Open Data Publication	Dataset: Kolodziejczyk et al., 2021 Publication: Gaillard et al., 2016
~~9~~	~~Scripps institution of oceanography (SIO) – Roemmich-Gilson Argo Climatology~~	~~UCSD SIO Argo website: https://sio-argo.ucsd.edu/RG_Climatology.html~~	~~Publication: Roemmich and Gilson, 2009~~
~~10~~9	Met Office Hadley Centre observations datasets: EN4.2.2. (c14)	MetOffice website: https://www.metoffice.gov.uk/hadobs/en4/download-en4-2-2.html	Publications: Good et al., 2013; Cheng et al., 2014; Gouretski and Cheng, 2020.
~~11~~	~~JAMSTEC Argo product - Grid Point Value of the Monthly Objective Analysis using the Argo data (MOAA GPV), version 2021~~	~~JAMSTEC website : https://www.jamstec.go.jp/argo_research/dataset/moaagpv/moaa_en.html~~	~~Publication: Hosoda et al., 2010~~
~~12~~10	NOAA (National Oceanic and Atmospheric Administration) - NCEI (National Centers for Environmental Information) product	NCEI-NOAA website : https://www.ncei.noaa.gov/access/global-ocean-heat-content/	Publication: Levitus et al., 2012; Garcia et al., 2019
11	GLOBAL_OMI_OHC_area_averaged_anomalies_0_2000; Numerical models, In-situ observations, Satellite observations	EU Copernicus Marine Service Product, 2021.	Quality Information Document (QUID): von Schuckmann et al., 2021. Product User Manual (PUM): Monier et al., 2021
12	GCOS EHI Experiment 1960-2020	World Data Center for Climate at DKRZ	Dataset: von Schuckmann et al., 2022. Publication: von Schuckmann et al., 2023.
13	JPL GOHC change dataset from space data	https://zenodo.org/records/5104970	Publication: Hakuba et al., 2021

~~13~~14	CERES Energy Balanced and Filled (EBAF) TOA and Surface Monthly means data in netCDF Edition 4.2.	NASA Atmospheric Science Data Center	Dataset: DOELLING, 2023 Publications: Loeb et al., 2018; Kato et al., 2018.
15	Met Office Hadley Centre observations datasets: EN4.2.2.(l09)	MetOffice website: https://www.metoffice.gov.uk/hadobs/en4/download-en4-2-2.html	Publications: Good et al., 2013; Levitus et al., 2009.

Figure 1:~~-~~ Global ocean heat content change over 1993-2022 depicted by the LEGOS-Magellium space geodetic dataset (red curve) and the GCOS dataset available until 2020 (purple curve). The LEGOS-Magellium dataset is characterised by its standard uncertainty envelope ~~[16-84%].~~(68% confidence level). The ocean surface considered for the LEGOS-Magellium dataset is comparable to that of the GCOS ensemble (von Schuckmann et al., 2023). Trends are estimated ~~over 1993-2020~~ at 5-95% confidence interval level and refer to the top-of-atmosphere surface.

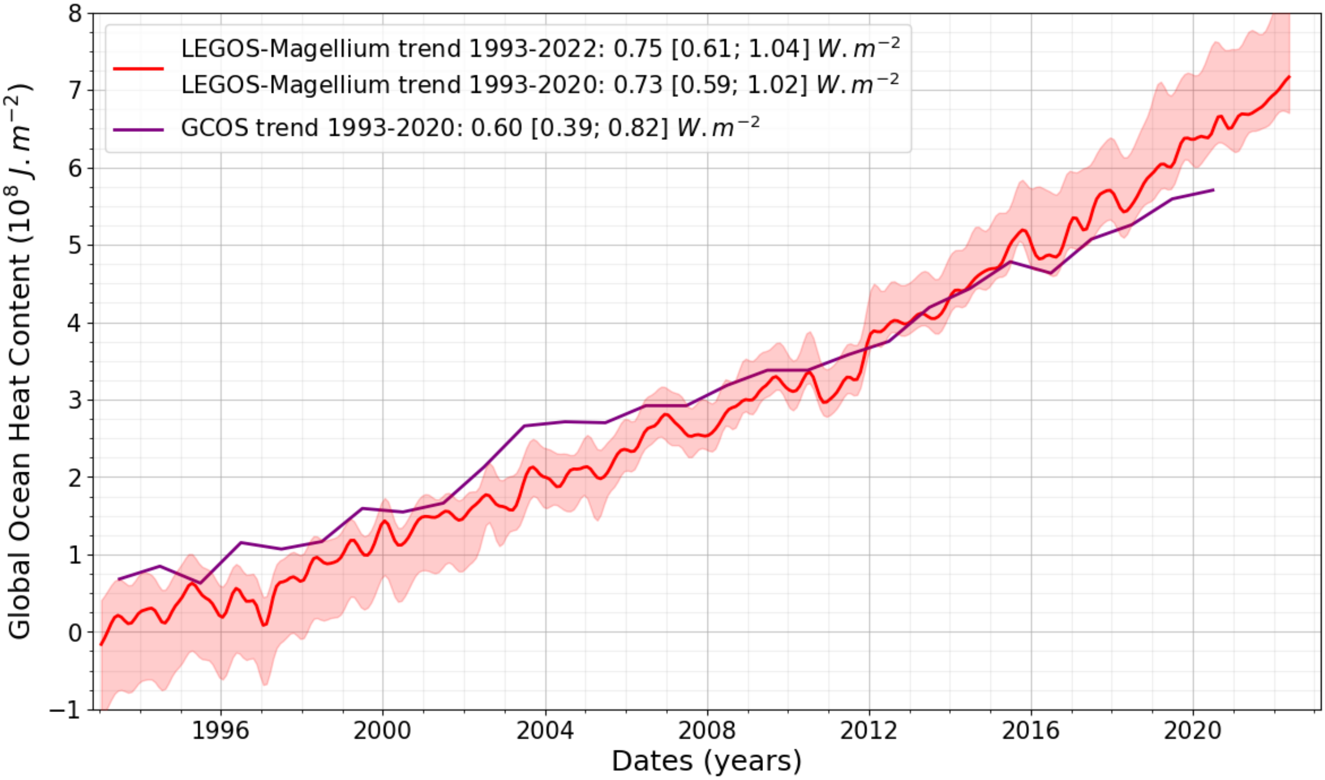

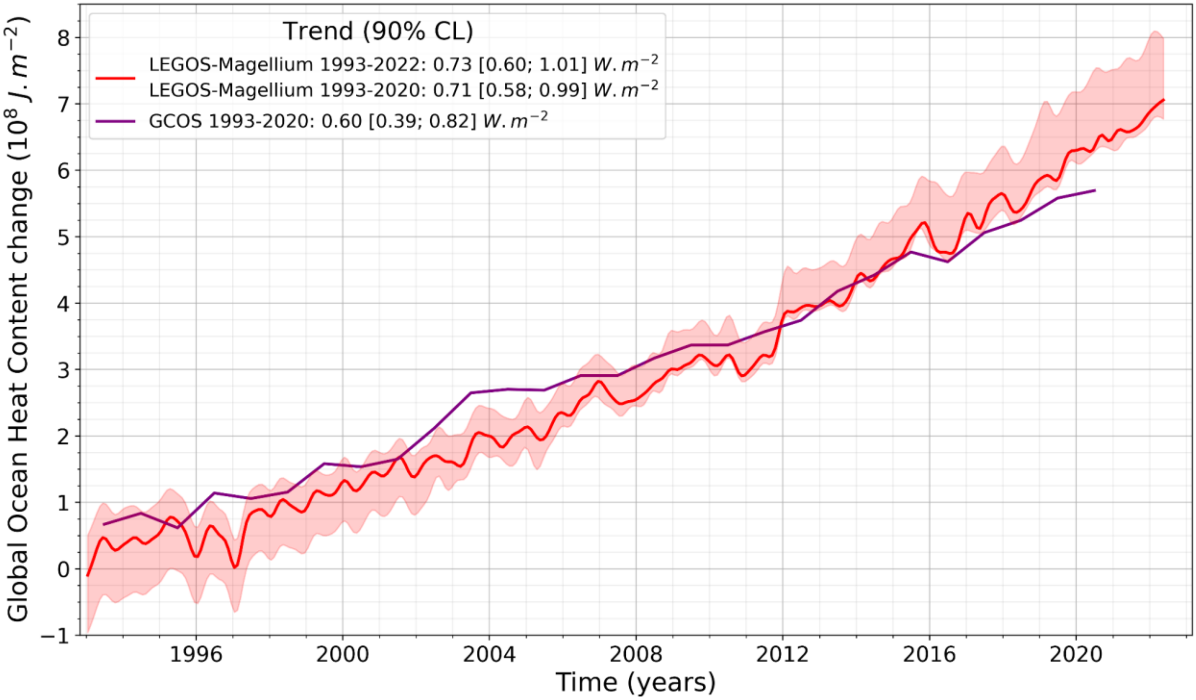
Trend (90% CL)
LEGOS-Magellium 1993-2022: 0.73 [0.60; 1.01] $W.m^{-2}$
LEGOS-Magellium 1993-2020: 0.71 [0.58; 0.99] $W.m^{-2}$
GCOS 1993-2020: 0.60 [0.39; 0.82] $W.m^{-2}$
Global Ocean Heat Content change ($10^8\,J.m^{-2}$)
Time (years)

Figure 2: Global ocean heat content (GOHC) trends over the period 2005-2019 from the LEGOS-Magellium (red) and JPL (blue) space geodetic ~~dataset (red),~~datasets, the GCOS ensemble (purple), ~~Argo~~in-situ-based GOHC change time series (brown tones), and the ~~3~~2 CMEMS indicators (green~~/blue~~ tones). ~~The~~ Trends are computed from annual time series and refer to the top-of-atmosphere surface and the indicated trend intervals correspond to the [5-95~~%~~%] confidence interval level~~. ISAS20, SIO, EN4.c14, JAMSTEC, NOAA, CORA and ARMOR3D GOHC trend uncertainties correspond to the adjustment error by the ordinary least squares method~~.

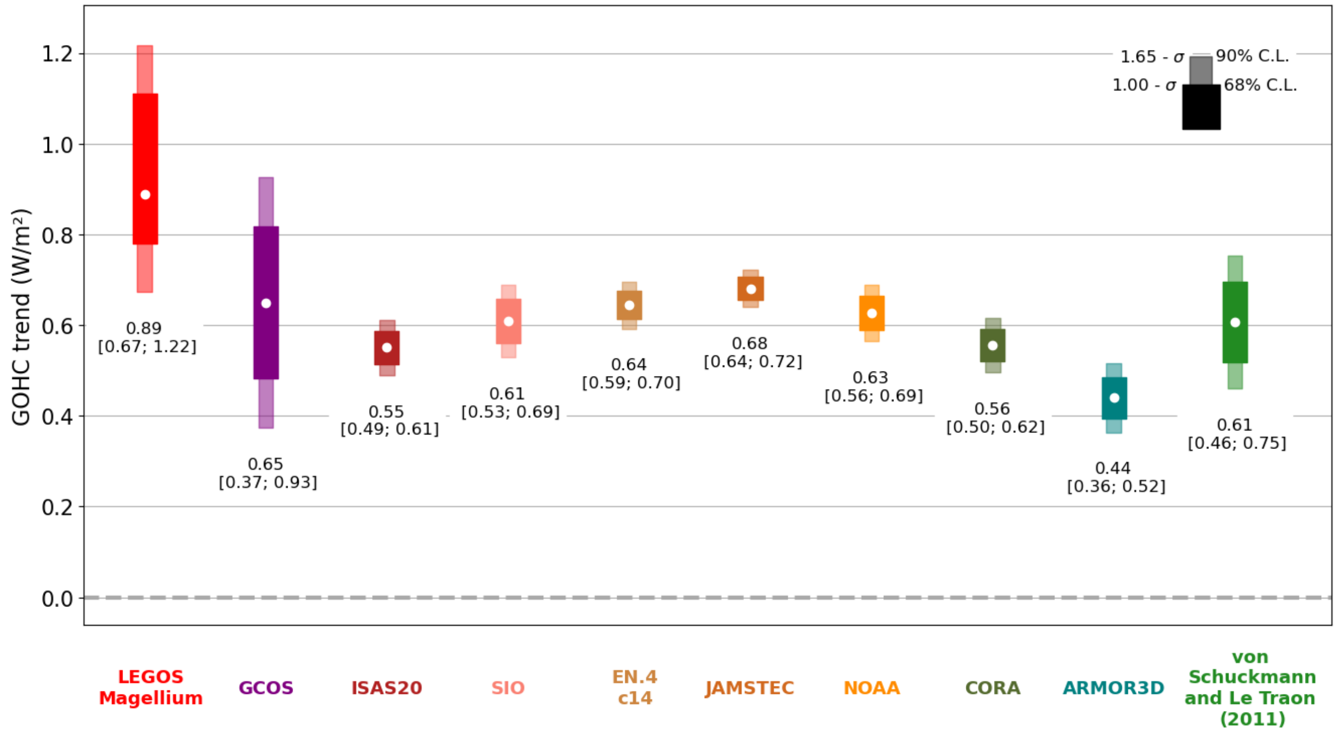

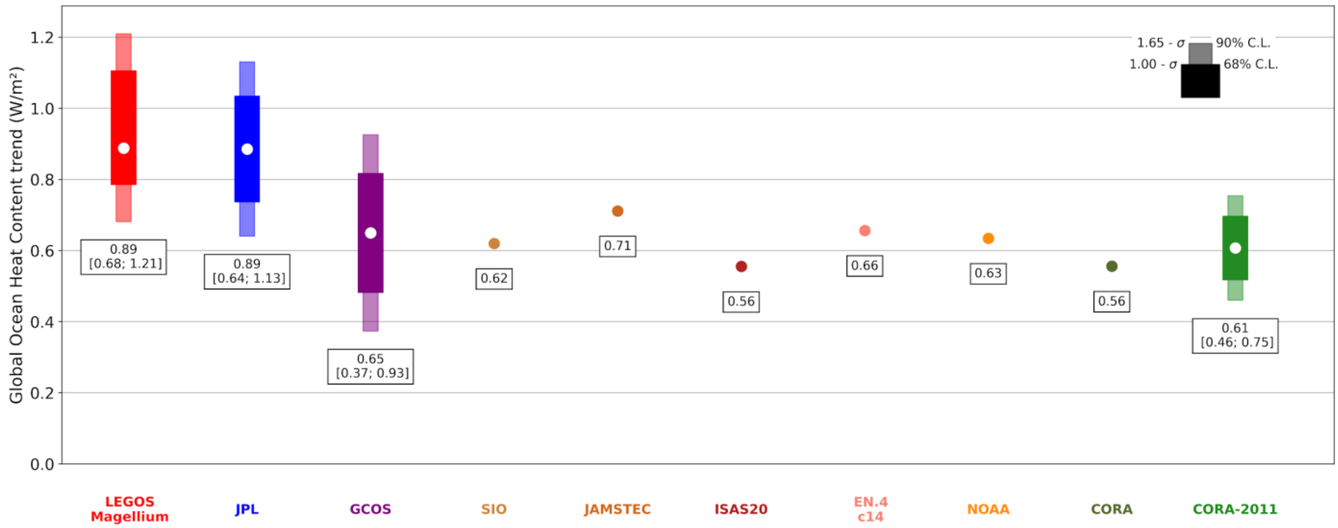
Global Ocean Heat Content trend (W/m²)
0.0
0.2
0.4
0.6
0.8
1.0
1.2
1.65 - σ 90% C.L.
1.00 - σ 68% C.L.
0.89 [0.68; 1.21]
0.89 [0.64; 1.13]
0.65 [0.37; 0.93]
0.62
0.71
0.56
0.66
0.63
0.56
0.61 [0.46; 0.75]
LEGOS Magellium
JPL
GCOS
SIO
JAMSTEC
ISAS20
EN.4 c14
NOAA
CORA
CORA-2011

Figure 3: Earth energy imbalance (EEI) time series derived from the LEGOS-Magellium space geodetic approach (~~black~~red curve), GCOS dataset (purple curve) and from satellite CERES measurements (~~blue~~black curve) over 1993-2022. A 3-year filter is applied to the space geodetic GOHC before derivation into EEI. CERES time series is also filtered at 3 years for comparison. Standard uncertainty envelope ~~[16 % 84%]~~(68% confidence level) is shown for the space geodetic dataset in ~~grey~~light red. EEI trends are given for each dataset on their common availability period 2000-2020 and ~~uncertainties~~refer to the top-of-atmosphere surface. Uncertainties are estimated ~~at~~ with a [5-%-95~~%~~%] confidence interval level.

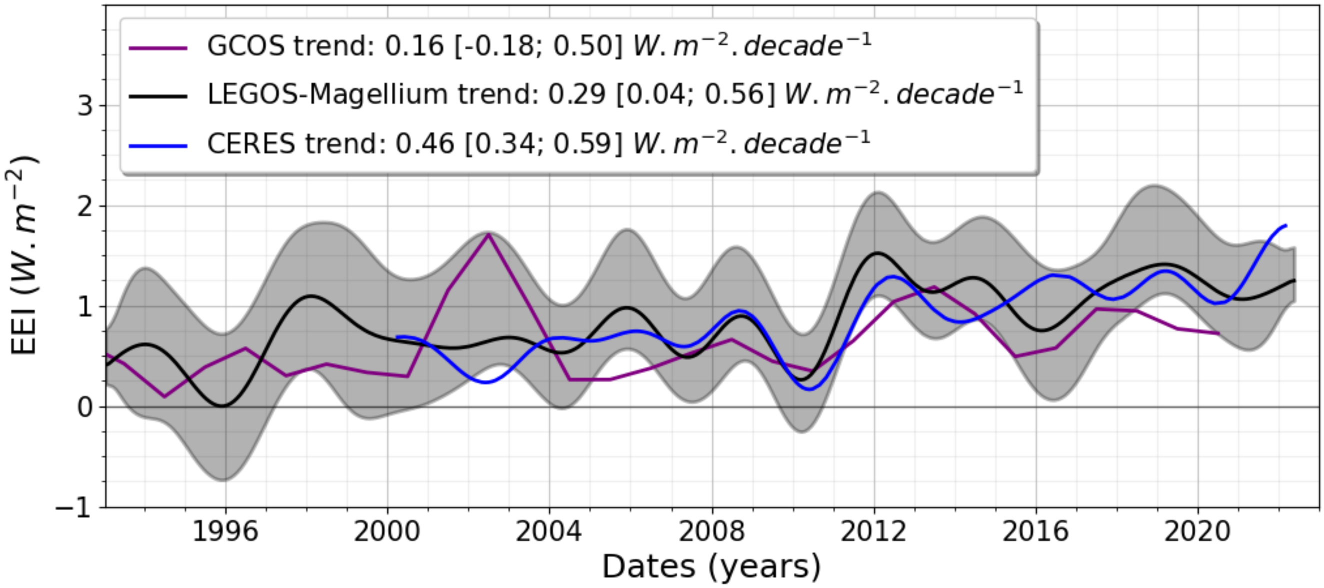

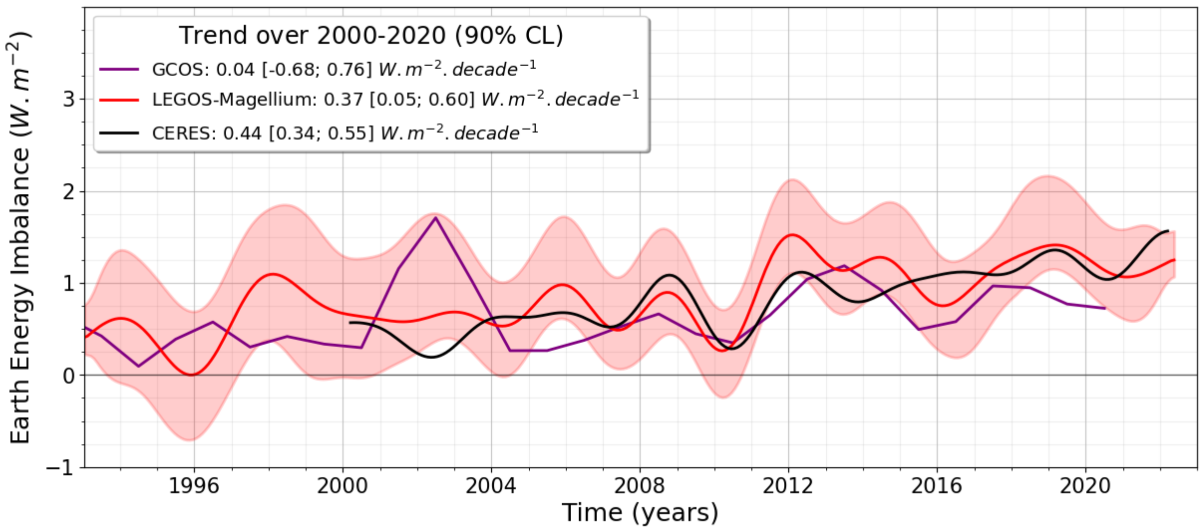

Trend over 2000-2020 (90% CL)
GCOS: 0.04 [-0.68; 0.76] $W.m^{-2}.decade^{-1}$
LEGOS-Magellium: 0.37 [0.05; 0.60] $W.m^{-2}.decade^{-1}$
CERES: 0.44 [0.34; 0.55] $W.m^{-2}.decade^{-1}$
Earth Energy Imbalance ($W.m^{-2}$)
Time (years)

Figure 4: Comparison of Earth energy imbalance (EEI) interannual variations with respect to the CERES dataset (~~blue~~black star) on the 2005-2019 period. Taylor diagram gathering the correlation Pearson coefficient, the centred root means square (W m-2) and the standard deviation (W m-2) for the LEGOS-Magellium ~~dataset~~ (red), ~~the~~JPL (blue), GCOS ~~dataset~~ (purple), ~~the Argo~~in-situ-based EEI ~~time series~~ (brown tones), and ~~the~~ CMEMS indicators (green~~/blue~~ tones). Results refer to the top-of-atmosphere surface.

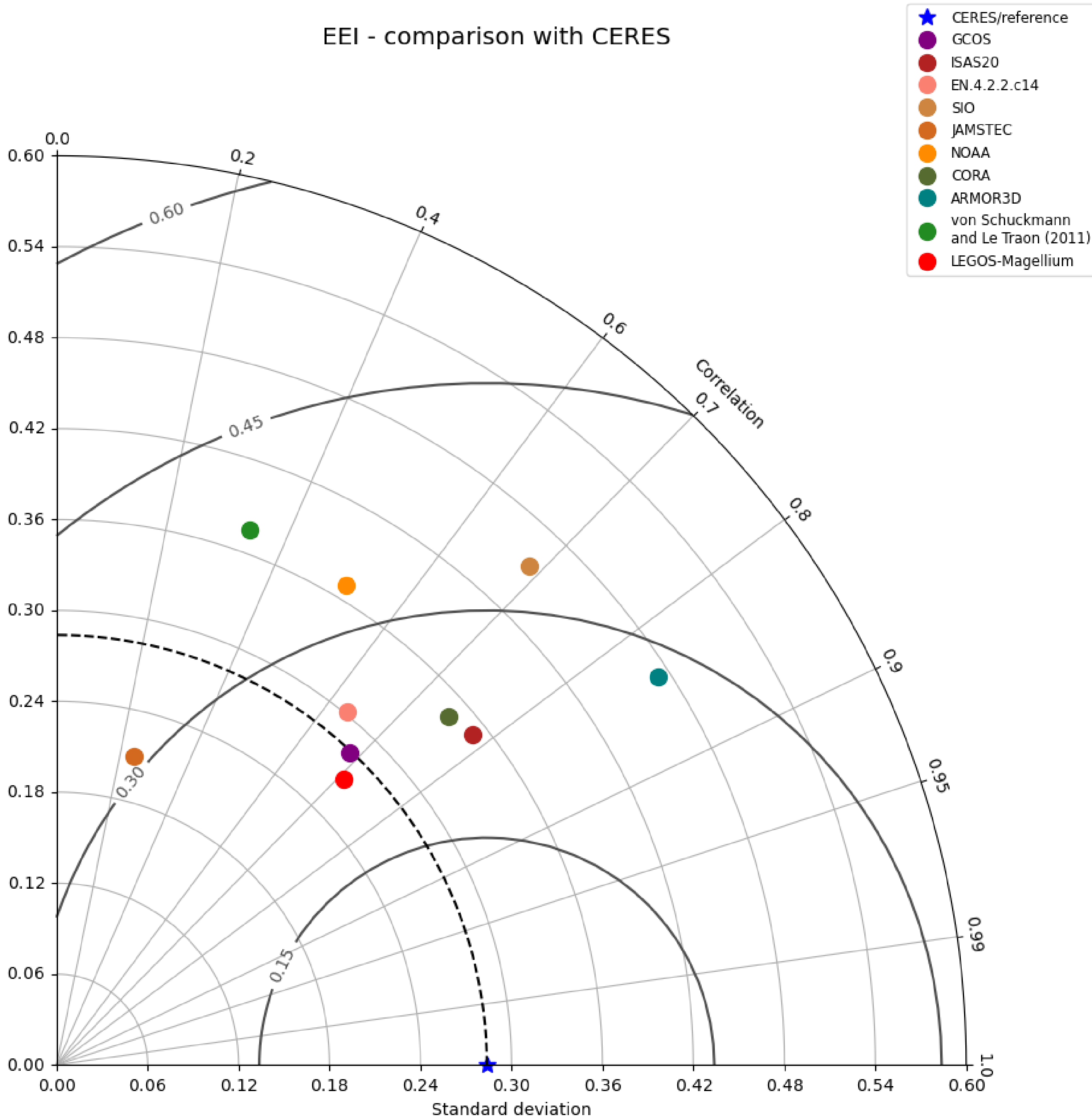
EEI - comparison with CERES
CERES/reference
GCOS
ISAS20
EN.4.2.2.c14
SIO
JAMSTEC
NOAA
CORA
ARMOR3D
von Schuckmann and Le Traon (2011)
LEGOS-Magellium
Correlation
Standard deviation
0.00
0.06
0.12
0.18
0.24
0.30
0.36
0.42
0.48
0.54
0.60
0.0
0.2
0.4
0.6
0.7
0.8
0.9
0.95
0.99
1.0
0.15
0.30
0.45
0.60

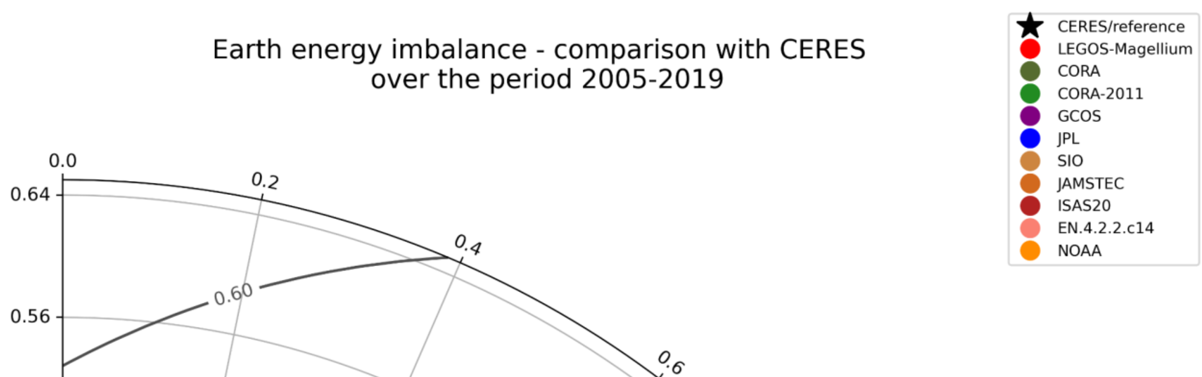
Earth energy imbalance - comparison with CERES over the period 2005-2019
CERES/reference
LEGOS-Magellium
CORA
CORA-2011
GCOS
JPL
SIO
JAMSTEC
ISAS20
EN.4.2.2.c14
NOAA
0.0
0.2
0.4
0.6
0.64
0.56
0.60